Eur. Phys. J. B **47**, 305–314 (2005)
DOI: 10.1140/epjb/e2005-00326-9

THE EUROPEAN PHYSICAL JOURNAL B

Contactless gating, surface charging and illumination effects in a buried $Al_{0.24}Ga_{0.76}As/GaAs$ quantum well structure

M. Biasini[1,2,a], R.D. Gann[1], L.N. Pfeiffer[3], K.W. West[3], X.P.A. Gao[4], B.C.D. Williams[1], J.A. Yarmoff[1], and A.P. Mills, Jr[1]

[1] Department of Physics, University of California Riverside, Riverside CA 92521, USA
[2] ENEA, Via Don Fiammelli 2, 40129 Bologna, Italy
[3] Bell Laboratories, Lucent Technologies, Murray Hill NJ 07974, USA
[4] Los Alamos National Laboratory, Los Alamos, NM 87545, USA

Received 29 April 2005 / Received in final form 11 July 2005
Published online 11 October 2005 – © EDP Sciences, Società Italiana di Fisica, Springer-Verlag 2005

Abstract. The conductivity of an $Al_{0.24}Ga_{0.76}As/GaAs$ quantum well was studied as a function of the surface charge generated by electron bombardment of the sample in the absence of an externally applied surface electric field. Under a suitable rate of electron irradiation, it was possible to completely shut off the conductive channel, implying a surface density $n = 2.5 \times 10^{11}$ el/cm^2. Light illumination quenches the increase of the resistivity, apparently due to photoemission from the metastable surface states. Upon turning off the electron bombardment the surface charge on adsorbed layers of xenon and water at 8 K decays in room temperature darkness with a lifetime $\tau = 0.30 \pm 0.02$ s. The average charging efficiency, is $\mu_0 \simeq 0.001$. Surface charging is shown to be an effective method for *contactless* gating of field effect devices.

PACS. 73.20.-r Electron states at surfaces and interfaces – 73.40.-c Electronic transport in interface structures – 71.55.Eq III-V semiconductors

1 Introduction

Charging phenomena of dielectric surfaces involve fundamental processes such as quantum sticking or resonant trapping [1–3], and have a variety of applications. Unlike the case of charging a surface by a gate potential, a surface which has no applied electric field can only be charged by electrons taking up residence in metastable surface or near surface states [4–8]. The mechanisms leading to the local charge imbalance and localization are only poorly understood. Various techniques have been developed to measure charge trapping and its effects, extending from indirect measurements, such as thermally or optically stimulated discharges, to direct determination of the surface potential.

The method adopted in this work for investigating surface charging has potential semiconductor device applications. It is well known that in MOSFET-type devices the insulating layer inserted between the gate (G) and the source-drain (SD) channel allows control of the conductive properties of the device via the electrostatic field between the gate and the channel. Typically, this field is provided by an external voltage connected to the gate with an ohmic metal contact. We propose to replace the power supply and metallic gate with an electrostatic charge induced by low energy electron bombardment of the semiconductor surface. In other words, the device will be gated by controlling the charge state of the surface. Note that this process does not perturb the material surface, unlike the case of MOSFET devices where a dielectric overlayer is deposited to isolate the gate from the conducting channel. Thus, a surface with particular intrinsic electronic states could be maintained in pristine condition as the gate is operated. Gating a field effect device by impinging its surface with an electron beam could be useful in specific situations where external conditions prevent the application of metal contacts to the gate or where the gating will be applied to a surface that must be accessed by some microscopic probe. Such *contactless gating* could be especially useful for devices requiring the utmost mobility [9], and for organic devices for which the electrons are confined in the topmost layer of molecules [10].

The quantity measured in this arrangement is the resistance of the SD channel and its time evolution at the turn on and off of the electron gun. The time evolution should directly reflect the charging and discharging of the

[a] e-mail: biasini@physics.ucr.edu

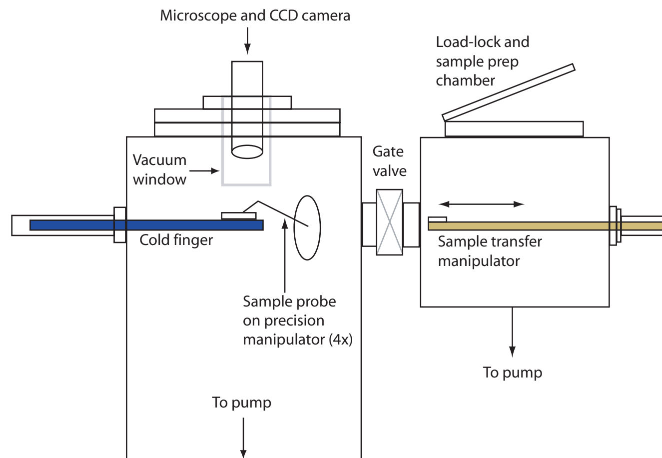

Fig. 1. Schematic diagram of the UHV chamber utilized for the experiments.

external surface. This information can then be used to study the metastability of the surface charge states. Moreover, if the SD channel involved conduction through the surface states of a particular material, this setup could be used as a means for investigating surface transport properties.

To investigate the feasibility of this method, we have chosen a well characterized $Al_{0.24}Ga_{0.76}$AlGas quantum well (QW) device. The density of the two dimensional electron gas (2DEG) which forms in the QW is controlled by charging the outer surface, which is only 200 nm above the QW.

The charging process is investigated under different surface preparations. We tested i) the bare (untreated) surface of the sample, consisting of an undoped GaAs thin layer; ii) the coverage of a perfect dielectric consisting of solid Xe; and iii) an additional coverage of ice deposited onto the Xe substrate. The different treatments had the purpose of A) optimizing the charge trapping and, consequently, maximizing the gating effect; and B) studying the material dependence of the transient processes (time dependence of the charging and the eventual discharging). These choices were motivated by previous findings that the addition of ice onto a rare gas substrate enhances the charging process [4,5].

In reference [11] we demonstrated the feasibility of the method for gating a QW. In the present work we discuss the charging of the surface of a dielectric in more detail, pointing out how this process is affected by external conditions such as illumination with infrared radiation or visible light.

This paper is organized as follows. In Section 2 the experimental method and the composition of the sample are described. In Section 3 we report the measurements and discuss their relevance. In Section 4 we summarize the results and outline possible improvements and developments of the contactless gating method.

2 Method

A custom UHV chamber was modified for in situ surface transport measurements at low temperature (see Fig. 1). Samples are transferred through a load lock into the main chamber and placed in contact with the cold finger of a liquid He cryostat. Pressures on the order of 10^{-11} torr and temperatures down to 6 K can be attained. Four precision x-y-z manipulators, each ending in a thin ($\simeq$100 μm) tungsten microprobe, are used for electrical contact. Contact of the microprobes to the sample is made while being observed by a CCD camera fitted with a microscope lens. The sample resistance is measured either with a standard four point method or, when only two microprobes are available, by comparing the voltage drop across the sample with that of a calibrated resistor connected in series with the sample. The sample temperature is measured via a silicon diode temperature sensor in thermal contact with the sample.

Two electron guns were utilized in the course of the experiments. The first consisted of a thoriated tungsten filament and two extracting electrodes. The guiding of the electrons onto the sample was obtained simply by biasing the filament negatively (0 to 30 V) with respect to the sample and the whole chamber assembly. This gun succeeded in gating the device for biasing voltages greater than 35 V.

A later setup utilized a Kimball physics ELG-2 electron gun to maintain a constant focal plane position and spot size (2 mm diameter) for electron energies in the range from 10 eV to 1000 eV. The highest electron beam current was obtained for an energy of 160 eV. The gun was directed against a 10×15 mm^2 304 stainless steel plate located at $\simeq$10 mm from the sample, such that the secondary electrons re-emitted from the plate were utilized for the bombardment of the sample. Low energy secondary electrons typically have an asymmetric energy distribution with a maximum at a few eV, a full width at half maximum, (FWHM) $\simeq$ 10 eV and a secondary emission yield, δ_{max}, defined as the average number of secondary electrons emitted per incident electron, of $\delta_{max} \simeq 1$, for an incident electron energy on the order of 100 eV [13,14]. Note, however, that the shape of the distribution and δ_{max} are very dependent on the degree of contamination of the emitting surface [13]. The metal plate emitting the secondary electrons was either grounded ($V_b = 0$ V) or biased with a negative voltage ($V_b = -25$ V). A negative bias enables the energy spectrum of the bombarding electrons to be shifted to higher energies. The gun was switched on and off and by an FET (switching time $\simeq$ 100 ns) which controlled the voltage of an electrostatic element within the gun assembly.

The electron bombardment was either carried out on the bare surface of the sample or after depositing a selected number of layers (typically 10 to 100) of Xe and/or water. Deposition was carried out by introducing gases into the main chamber through sapphire leak valves. The amount of material deposited was determined by the product of the opening time of the valve and the increase of pressure during the operation. The number of deposited

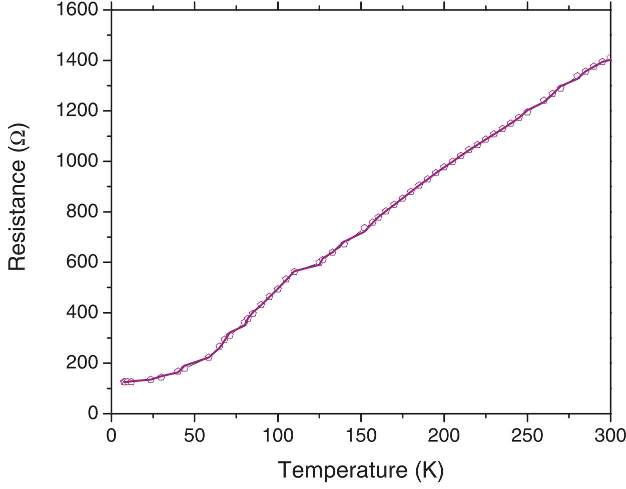

Fig. 2. Typical behavior of the resistance vs. T of the $Al_{0.24}Ga_{0.76}As/GaAs$ samples. Measurements were carried out under continuous illumination.

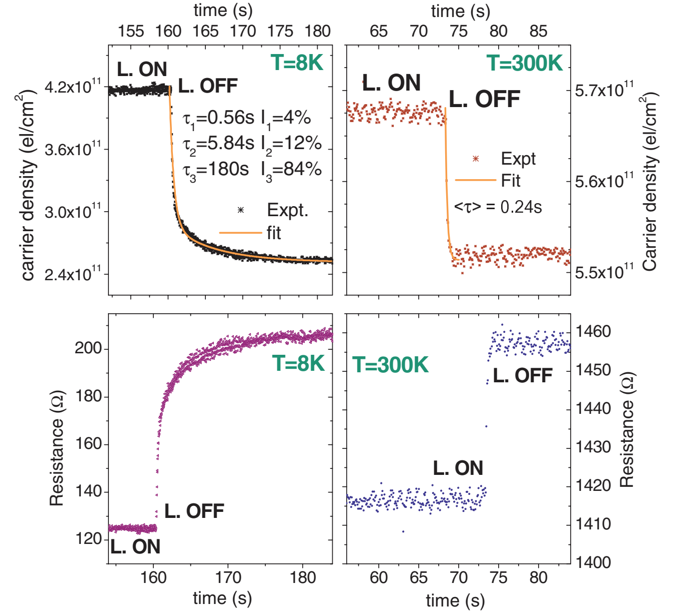

Fig. 3. Bottom panels: The recovery of the darkness resistance as a function of time at the turn off of the light at $T = 8$ K and $T = 300$ K (L.ON: light on; L.OFF: light off). Top panels: Conductance ($G = 1/R$), expressed in terms of the carrier density obtained from Hall measurements. The continuous lines are obtained by fitting the carrier density at $T = 8$ K and $T = 300$ K with three and one exponential time decays, respectively. Note that the absolute values of the time scales of the figure refers simply to the subset of data shown and have no special physical meaning.

layers was estimated under the assumption that i) the sticking coefficient of the gas striking the sample was unity; and ii) the deposition was uniform over the surface [12].

Samples were grown on a 500 μm thick GaAs(100) wafer. Delta doping layers of Si dopants were symmetrically placed above and below the 80 nm thick $Al_{0.24}Ga_{0.76}$ barriers. The GaAs QW, located between the barriers, was 30 nm thick. The sign of the Hall constant indicated that the Si delta dopant acts as a *donor*, consistent with a growth direction parallel to [100]-type crystallographic axes [17]. The 2DEG density and the mobility of the carriers were determined in separate experiments by measuring the Hall constant and the Shubnikov-de Haas (SdH) oscillations of the resistivity as a function of an applied magnetic field. The latter measurement was performed in a ^{3}He/^{4}He dilution refrigerator. The density of carriers were 2.5×10^{11} el/cm^2 and 5.5×10^{11} el/cm^2 at $T = 4$ K and $T = 300$ K, respectively. The mobility at 4 K was $\mu = 9.5 \times 10^6$ cm^2/V s.

Typical sizes of the cleaved samples were 4×4 mm^2. The electrical contact between the W microprobes and the buried QW was obtained by depositing up to four indium patches onto the surface. The sample was then annealed at 450 °C in flowing hydrogen to induce the diffusion of indium into the sample. Note that such annealing temperature is much smaller than the temperature at which the intermixing of the heterojunction begins [18] ($T \simeq 800\,°$C). After annealing, the resistance between any two indium patches showed typical metallic behavior (see Fig. 2).

3 Results and discussion

3.1 Reversible photoconductivity

Since illumination alters the effectiveness of contactless gating of the buried QW samples chosen for these measurements, it is important to describe the effect of illumination on the resistance prior to the electron bombardment. All the samples measured showed large photoconductivity effects at $T = 8$ K (the typical temperature of the measurements) and clearly observable ones even at room temperature. The lower panels of Figure 3 show the resistance through the QW as a function of time as the illumination is turned off. The light was produced from a tungsten-halogen lamp shining directly onto the sample through a glass viewport (when the lamp was off the sample was in almost total darkness). The electron gun was always off during these measurements. Interestingly, whereas at room temperature the resistance reverts to its darkness value almost immediately after the turn off of the light, a much slower recovery is observed at 8 K.

The time dependence of the conductance G ($=1/R$) can be fit by the sum of up to three exponential decays, as shown in the upper panels of Figure 3. We find it appropriate to express G in terms of the carrier density obtained in darkness from previous Hall measurements, assuming that the light does not affect the electron mobility. At $T = 8$ K, a high intensity slow decay ($\tau_3 = 180$ s) is superimposed on low intensity shorter decays (see values in Fig. 3). On the other hand, at $T = 300$ K the fall time of the conductance at the turn off of the light is less than 1 second and is possibly due simply to the time needed for the illumination to turn off. Whereas it is plausible that the shortest component observed at the turn off of the light

at $T = 8$ K ($\tau_1 \simeq 0.5$ s) is also due to the cooling time of the halogen lamp, the two longer components should be ascribed to some (de)activated process within the sample.

We emphasize that the decrease/increase in resistance is completely reversible at the turn on/off of the light, within the time constants discussed above. Therefore, this phenomenon is completely different from the persistent photoconductivity (PPC) thoroughly discussed in the literature [19]. In the latter case, a popular mechanism invoked to explain the PPC has been the release of charge under illumination by the so-called "DX" centers [20]. These traps are donors (e.g., Si atoms) which undergo lattice relaxation and, instead of releasing an electron into the conduction band (as normal donors should do), trap an additional electron, becoming negatively charged. Under illumination the DX center can release these electrons into the conduction bands. On the other hand, the capture of electrons into a DX center is thermally activated. Therefore, retrapping can be energetically unfavorable at low temperature. The activation energy increases with the decrease of the Al concentration in the $Al_xGa_{1-x}As$ layer. At the concentration of our sample the activation energy is $E_a \simeq 0.45$ eV, making the trapping at $T = 8$ K practically impossible [21]. Therefore, the mechanism that gives rise to the reversible photoconductivity observed here cannot be ascribed to the DX centers. Moreover, the long time constants observed, which are many orders of magnitude longer than a typical carrier transit time ($t_{\text{transit}} < 10^{-8}$ s), rule out a simple mechanism where the increase in conductivity under illumination is due to electron-hole excitations and their consequent recombination when the light is turned off.

Note that low temperature reversible photoconductivity (at $T = 1.7$ K), superimposed onto the PPC, has been observed in Si delta-doped $In_{0.2}Ga_{0.8}As$/GaAs quantum well structures with characteristic recovery times of minutes [22]. Whereas the authors in reference [22] propose a mechanism for the PPC in terms of photogenerated electrons detrapped by light from deep centers, they do not attempt any explanation for the reversible photoconductivity.

In a way, the data of Figure 3 show therefore two rather contrasting experimental findings.

i) On the one hand, the increase in the resistance when the light is turned off requires that either the mobility or the *number of carriers decreases*.

ii) On the other hand, the long time taken by the sample to recover the dark resistance suggests the existence of a thermally activated process leading to the *release of charge from an unknown shallow trap*. A crude estimate of the binding energy of the trap, E, can be obtained adopting the simple relation $1/\tau \propto e^{-E/k_B T}$ (where k_B is the Boltzmann constant, T the temperature and τ is the trap lifetime), and employing the two available values of the lifetime, $\tau \cong 180$ s for $T = 8$ K, and $\tau \cong 0.2$ s for $T = 300$ K [23], displayed in the upper panels of Figure 3. The energy obtained, $E = 5 \pm 1$ meV, is a typical activation energy for impurity levels in semiconductors [24].

A way to reconcile these two phenomena is to assume that, at the turning off of the light, the carriers thermally released from the shallow traps (possibly due to impurity levels) recombine in the depletion layer causing a decrease of the band bending and consequently of the density of the conduction carriers in the QW. Subsequent illumination produces electron-hole pairs from the unlimited valence band reservoir which refill the shallow traps and ionize the depletion layer, which reverts to the higher conductivity.

3.2 Resistance vs. electron bombardment

Figure 4A shows the low temperature sample resistance ($T = 8$ K) under the action of the electron gun (off/on). Measurements were performed on the bare sample surface, consisting of a 10 nm thick undoped GaAs layer, or after depositing $\simeq$ 100 layers of Xe or a double structure of Xe and H_2O molecules (for a total of $\simeq$200 layers). The resistance increases considerably under the electron bombardment, as would be expected under the application of a traditional gate [15]. The increase in resistance is well understood and it has been utilized in the last decade to control the density of the 2DEG [25]. Namely, the electric field produced by the surface charge counterbalances the one caused by the charge of the depletion layer of the Si delta dopant which "locks" the 2DEG in the QW. The result is a decrease in the carrier density and, in turn, an increase of the resistance.

The typical electric field E that completely shuts off the conducting channel is $E = \sigma/K\epsilon_0$, where ϵ_0 is the dielectric constant, σ the 2DEG charge density, and K is the permittivity. Using $\sigma = 2.5 \times 10^{11}$ el/cm^2, $K \simeq 11$, and a distance between the surface and QW of $d = 200$ nm yields $V \simeq 1$ V. In the case of a partial shut off of the conducting channel, the surface charge density n_s can be estimated as the difference between the Gun off/Gun on 2DEG density, i.e.,

$$n_s = n_{\text{2DEG}}^{\text{OFF}} - n_{\text{2DEG}}^{\text{ON}} = n_{\text{2DEG}}^{\text{OFF}}(1 - R_0/R_1), \qquad (1)$$

where $n_{\text{2DEG}}^{\text{OFF}}$ is the pristine 2DEG density (when the electron gun is off) and R_0 and R_1 are the gun off and gun on resistances, respectively. Figure 4B shows the surface charge density vs. time with the other parameters defined as in Figure 4A.

Figures 4A and B show that for all sample preparations the change in resistance is completely reversible with the switching of the electron gun. This implies that no permanent trapped states exist but only metastable ones. The largest change is observed with the bare sample surface under a plate voltage bias of $V_b = -25$ V. For all surface preparations a nonzero bias yields the largest increase in the resistivity. Most probably, the higher energy electrons can more easily overcome the negative space charge due to the slowest secondary electrons that pile up on the surface and hinder further bombardment of the sample.

The addition of rare gas or water layers, which were intended to favor a permanent electron trapping at the sample surface [4,5], seems to instead reduce the effect without changing considerably the time transients.

Table 1. Lifetime values of the decays of the surface charge density at the turnoff of the electron gun. Whereas τ_1 and τ_2 are the lifetimes of two independent exponential decays, τ_b, τ_s and I_3 refer to the model described by equations (2) and (3).

Surface	V_b (V)	τ_1 (s)	I_1 (%)	τ_2 (s)	I_2 (%)	τ_b (s)	τ_s (s)	I_3 (%)
bare	0	0.48±0.2	100±5	2±2	20±20	-	-	-
bare	−25	0.44±0.06	31±5	2.0±0.5	32±5	0.31±0.02	0.35±0.03	37±10
Xe	0	0.32±0.05	43±5	8±2	57±20	-	-	-
Xe	−25	0.38±0.05	10±2	8±2	69±10	0.31±0.03	0.36±0.04	21±5
Xe+H_2O	0	0.28±0.05	67±10	6±2	33±10	-	-	-
Xe+H_2O	−25	0.26±0.05	3±1	6±2	64±10	0.24 ±0.03	0.27±0.03	34±5

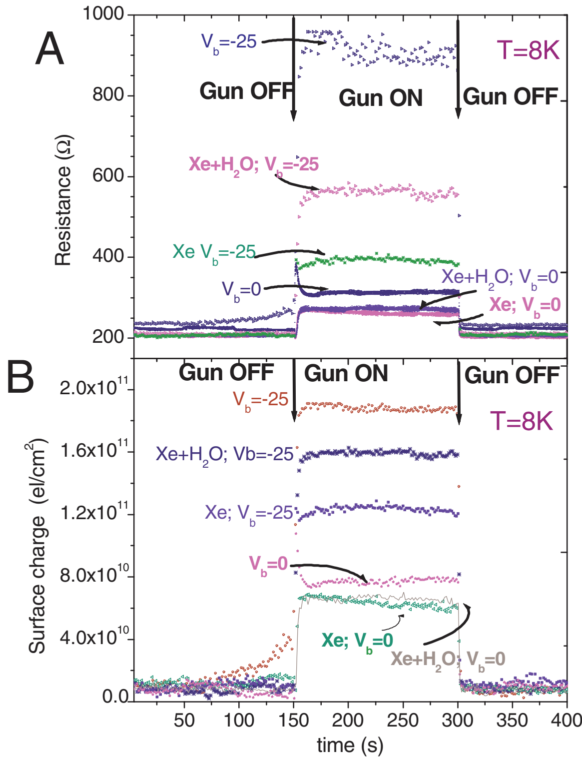

Fig. 4. A: Darkness resistance vs. time for various sample preparations and two electron gun energies (V_b = 0 V, V_b = −25 V) at the turn on/off of the electron gun. B: Predicted surface charge densities constructed as described in the text (see Eq. (1)). In Panel B, spectra were subjected to five point smoothing.

The decay of the surface charge at the turn off of the electron gun was analyzed by fitting its time dependence as a sum of two or three exponentials. For all cases, the largest amplitude decays have lifetimes in the range of 0.2–0.5 s. Longer low amplitude decays show a larger spread, but they have high fit uncertainties and are not completely reproducible (see Tab. 1). It is surprising that the different sample preparations lead to such similar decay times despite the difference in the magnitude of the effects.

To provide a better view of the transients, Figure 5 shows (in a semilog scale) a magnified time interval around the switch-off of the electron gun. It can be seen that the typical range of the time changes is much longer than the

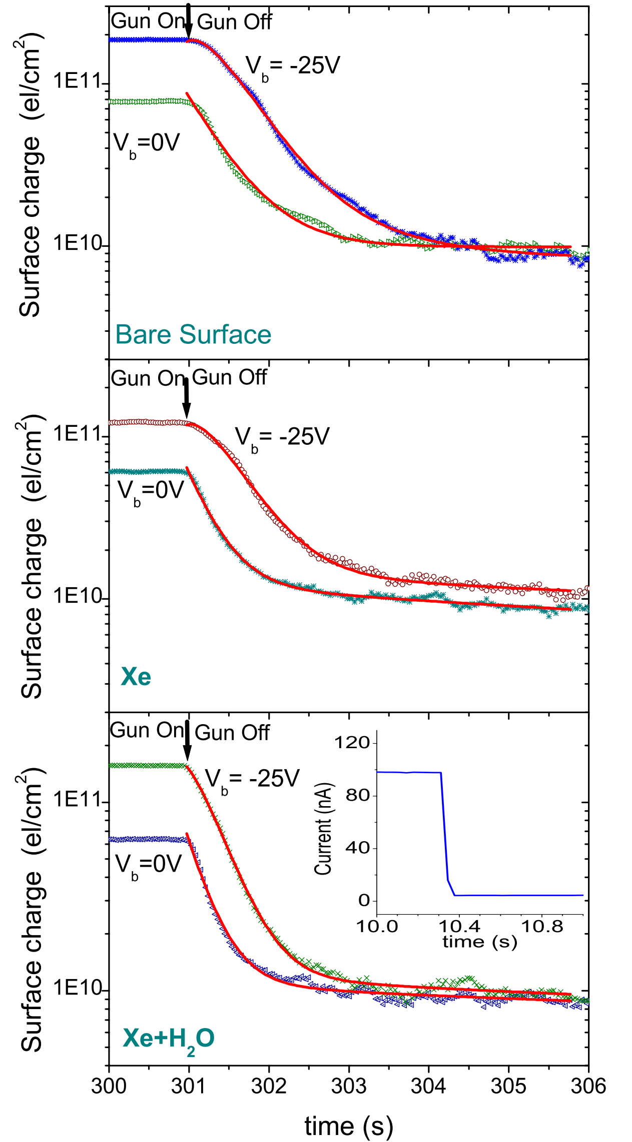

Fig. 5. Discharging of the surface at the turn off the electron gun under different surface treatments (from Fig. 4B nearby t = 300 s). Spectra were subjected to five point smoothing. The continuous lines are produced by fitting the decays with a sum of two exponentials, for the V_b = 0 V case, and with an additional function expressed by equation (3), for the V_b = −25 V case. The inset shows the typical time to switch off the electron gun current

switch-off time of the secondary electron current hitting the sample, shown in the inset. An interesting feature is the clear difference in the shape of the decay for the two biases of the secondary electron emitting plate ($V_b = 0$ V and $V_b = -25$ V) for the diverse surface preparations. Such difference was confirmed in different runs.

A simple model that can account for the time dependence of the decay is to assume that since the secondary electrons emitted by the plate set at negative bias ($V_b = -25$ V) reach the sample with a higher energy, they can be trapped into a *buried* state. The electrons trapped in the buried state decay into a surface state with rate λ_b and eventually are released in the vacuum with rate λ_s. The rate equations for the population of buried and surface states linked by this process, n_b and n_s, are

$$\begin{aligned} \dot{n}_b &= -\lambda_b n_b \\ \dot{n}_s &= \lambda_b n_b - \lambda_s n_s, \end{aligned} \qquad (2)$$

which can easily be solved. The sum of buried and surface charge, $n_T(t) = n_b(t)+n_s(t)$, contributes to the measured change in resistivity. The charge left on the sample at time t, $n_T(t)$, is then

$$n_T(t) = N_0 \left[\left(\frac{\lambda_s}{\lambda_s - \lambda_b} \right) e^{-\lambda_b t} - \left(\frac{\lambda_b}{\lambda_s - \lambda_b} \right) e^{-\lambda_t t} \right], \quad (3)$$

where N_0 is the number of electrons at $t = 0$ in the buried trap. Moreover, some electrons can be trapped immediately at the surface, as for the $V_b = 0$ V case, and reemitted directly in the vacuum.

The continuous lines shown in Figure 5 arise from fitting the time dependence of the experimental spectra with a sum of two independent exponentials for the $V_b = 0$ V bias and with the addition of the function shown in equation (3) for the $V_b = -25$ V bias. Although the complicated features of the spectra cannot be accounted fully by this simplified model, the overall agreement between data and fit is rather satisfactory. Lifetimes values are shown in Table 1. Interestingly, i) for each surface preparation τ_1 and τ_2 are almost independent of the plate bias, and ii) the surface lifetime τ_s coincides with τ_1, within the experimental error. This suggests that a fraction of higher energy electrons (absent in the $V_b = 0$ V case) does get trapped in deeper states. Note also the smaller values of all the lifetimes for the surface treated with Xe plus H_2O compared to the pure Xe or bare surface cases. A possible reason is the larger electron mean free path in Xe than in H_2O, which allows electrons to trap into deeper metastable states.

The onset of the charging process as a function of time is investigated by showing in Figure 6 (linear scale) a magnified time interval at the switch-on of the electron gun. Again, transients are much longer than a typical transient time of the electron gun current. It appears that in several cases the time changes of the resistance are non monotonic, unlike those of the turn off data presented in Figure 5. Moreover, the faint peaked structures shown in Figure 6, in the upper panel for $V_b = 0$ V and the middle panel for $V_b = -25$ V at $t \simeq 151.5$ s are not entirely reproducible. Such irregularities could be caused by changes

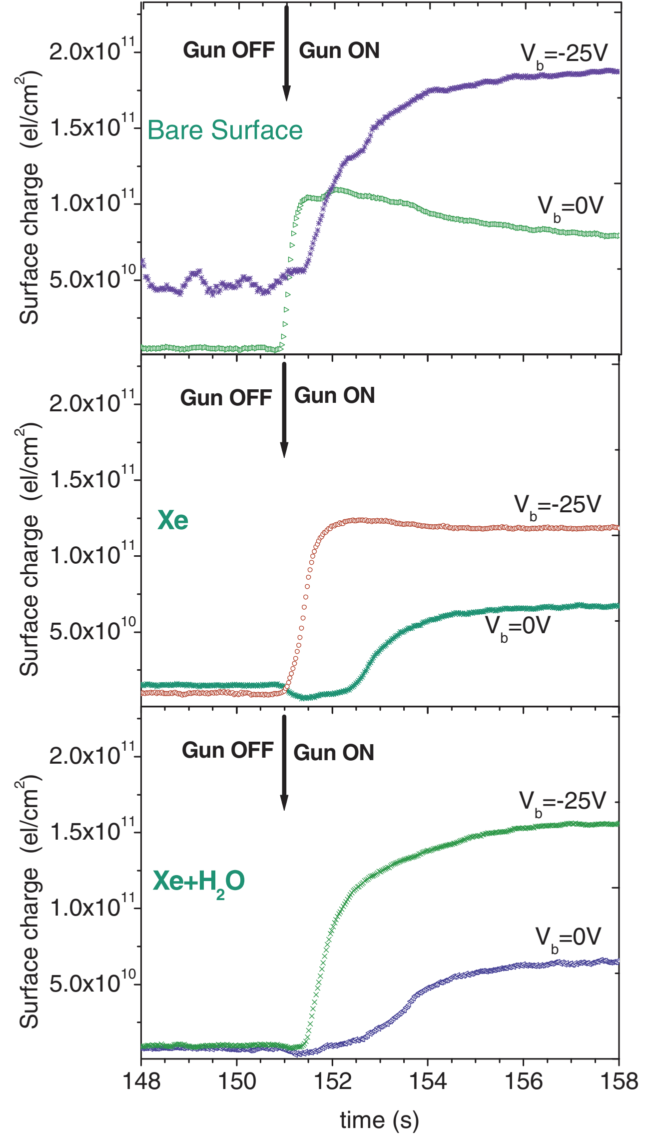

Fig. 6. Charging of the surface at the turn on the electron gun under different surface treatments (from Fig. 4B nearby $t = 150$ s). Spectra were subjected to five point smoothing.

in the state of the surface due to the desorption of contaminants by the electron beam.

The charging process as a function of time shown in Figure 6 reveals an onset time followed by a faster increase and a final saturation. From the final surface densities n, the typical time to reach saturation (typically $n \simeq 10^{11}$ el cm^{-2} and $t_s \simeq 2$ s, respectively) and the estimated total electron current density which reaches the sample $J_0 = 2^{2\pm1} \times 10^{13}$ el s^{-1} cm^{-2}, we can estimate a charging efficiency, μ_0, defined as the ratio of the charge collected by the surface to the beam current times the charging time, as

$$\mu_0 = \frac{n}{J_0\ t_0} = 10^{-3\pm0.3}.$$

The small value of μ indicates the difficulty of charging the surface of a dielectric.

Obviously, the process of charging using an external electron beam cannot proceed further when the build up of surface charge density σ produces a potential to ground as high as the highest energy of the impinging electrons, denoted as V_0, according to

$$V_0 = \frac{\sigma L}{K\epsilon_0}, \quad (4)$$

where L is the depth of the QW ($L = 200$ nm), which is grounded via one microprobe.

Note that equation (4) implicitly establishes a relation between energy of the impinging electrons, V_0 (referred to ground), the thickness of the sample L (having specific dielectric constant $K\epsilon_0$ and being in contact with a grounded sample holder) and the maximum charge density σ that can be deposited. In view of utilizing this method with novel materials, such as molecular organic crystals, this simple relation poses a serious limitation to the thickness of the samples. Obviously, the energy of the electrons should not be higher than a few eV if the aim is to deposit charge onto or nearby the surface. Low energy electrons are particularly important for use with these novel materials, which are often very sensitive to radiation damage [26]. Taking (as an upper limit) $V_0 = 50$ eV, $n = 2.5 \times 10^{11}$ el/cm^2 (the density of the 2DEG of this first attempt) and $K = 10$ one gets $L \simeq 10$ μm. Therefore, μm thick films are the upper limits for the effectiveness of this kind of *contactless gating*.

Furthermore, from equation (4), one can infer that by increasing the energy of the impinging electrons the time required to reach saturation should be longer if μ were constant. An alternative model description of the charging, following the guidelines of atomic adsorption-desorption processes, [4,12] would be to assume that the surface has a fixed number of traps n_0 and the voltage buildup is due to the filling of these traps. At time t the rate of charging is proportional to the free trap density, $n_f = n_0 - n$, i.e.,

$$\dot{n} = \frac{\mu I}{e}(n_0 - n), \quad (5)$$

where I is the electron current. Equation (5) can be integrated to give

$$n(t) = n_0(1 - e^{-\mu It/e}), \quad (6)$$

yielding for the voltage buildup at time t

$$V(t) = \frac{n_0(1 - e^{-\mu It/e})\ L}{\epsilon}. \quad (7)$$

However, Figure 6 shows that often neither the buildup of the charge follows the exponential behavior of equation (6), nor are the charging times proportional to the energy of the electrons. The most plausible explanation, as proposed in reference [4], is that the trapping efficiency is energy dependent. This assumption is very natural for the multiple traps model described by equation (2), which assumes two traps of different origin.

The problem of charging the surface of a dielectric has been thoroughly discussed by Sanche et al. [4]. These authors measured the so-called injection current through a thin dielectric layer (10–20 monolayers at most) deposited onto a metallic substrate. As the surface charges, the energy of the impinging electron beam need be increased to overtake the energy barrier originated by the trapped charge. Consequently, the injection curve shifts to higher energy.

Under particular conditions, Sanche et al. were able to trap charge for a long period of time. For example, a highly stable surface charge was attained for submonolayers of O_2 deposited on top of 10 monolayers of Kr. On the other hand, permanent charging was not observed on bare Kr [4]. In some cases [5] the trapping occurs only for near-zero kinetic energy electrons and is ascribed to the band structure of the underlayer. In our measurements, the charge quickly decayed as we did not produce the proper O_2/Kr structure, nor did we have access to a source of monochromatic, near-zero kinetic energy electrons.

Comparing these findings with the timing behavior of the charge density of our experiments it should be realized that the time constants shown in Table 1 differ little and the time decays are generally small. These findings suggest the trapping of the electrons in proximity of the surface of the medium under the effect of the image potential. This mechanism has been intensively studied theoretically and experimentally, although most of the experimental work was devoted to metallic surfaces [7,27–29].

The binding energies of the surface states for several metals were estimated to be within the range of 0.6–0.85 eV [28]. Addition of a few (one or two) monolayers of wide gap insulators, such as Xe, shifts the surface binding energy only slightly (for Ag(111) from 0.76 to 0.66 eV [30]). On the other hand, experimental values of surface bound states for solid insulators are much more scarce. The binding energies (E_b) calculated in reference [27] are much lower than the metallic cases. For example, for ^{4}He, $E_b = 0.7$ meV; for solid Ne, $E_b = 18$ meV; and for H_2, $E_b = 17$ meV.

These low binding energies hint that a possible cause for the charge release at the turn off of the electron gun is the blackbody radiation emanating from the chamber walls and then impinging the charged surface (the need to access the samples via the microprobes prevented the mounting of a radiative shroud). Although experimental values for the surfaces considered in this work are not available, it is plausible that black body radiation, whose maximum at 300 K is at $h\nu_{max} \simeq 0.13$ eV, is able to discharge the surface.

Therefore the surface charge labelled as n_s in equation (2) can be ascribed to the shallow trapped states caused by the image potential. On the other hand, we have no convincing models for the buried states conjectured in equation (2). Since they do not lead to permanent charging, they could simply be intermediate states of the dissociative attachment or resonant scattering reactions as predicted in references [4,5] which, due the interaction with vibrational levels of the surface (or near surface), do

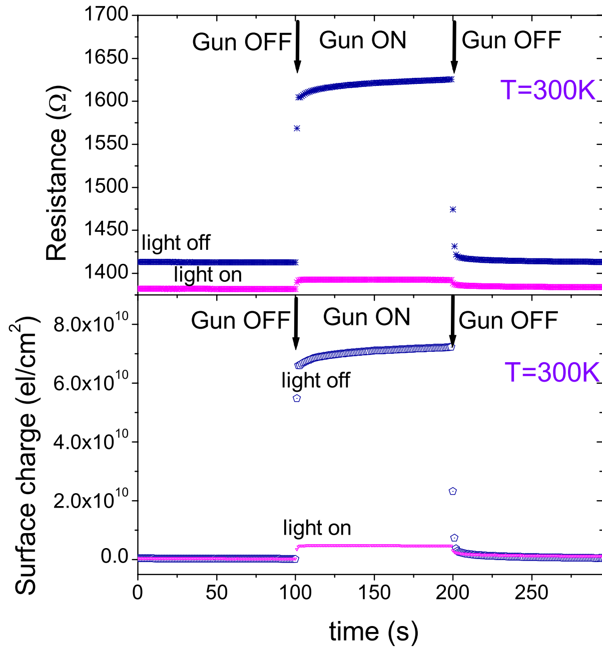

Fig. 7. A: Resistance vs. time at room temperature in darkness and under constant illumination. B: Predicted surface charge densities constructed as described in the text (see Eq. (1)). Electrons hitting the sample were biased with $V_b = -25$ V.

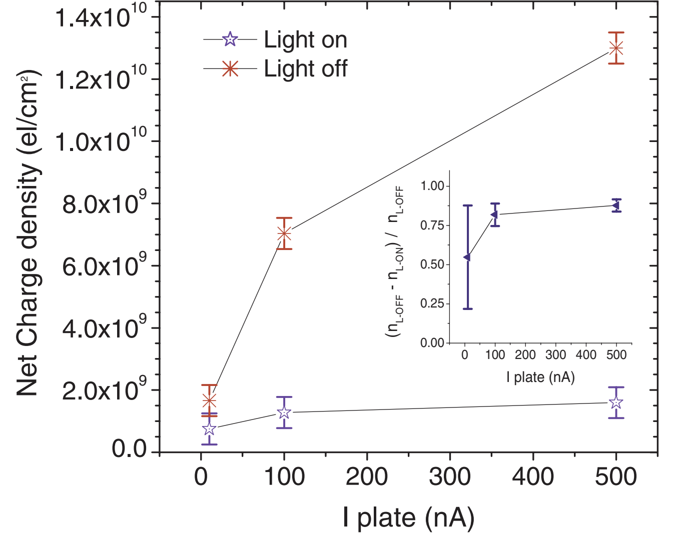

Fig. 8. Surface charge densities as a function of the electron gun current under darkness ($n^{\text{light off}}$) and illumination ($n^{\text{light on}}$). In the inset the ratio $(n^{\text{light off}} - n^{\text{light on}})/n^{\text{light off}}$ vs. gun current is plotted.

not lead to the permanent electron trapping. In any case, our empirical supposition is supported by the experimental trends of the decay curves.

3.3 Illumination effects

As mentioned above, previous measurements were performed in darkness. Figure 7 shows the result of the electron bombardment on the bare surface of the sample at room temperature. Although the effect is much smaller than at low temperature we observe a distinct increase in the dark resistance under electron bombardment. Figure 7 also presents the results of the same measurements, under constant illumination [31], for $V_b = -25$ V. Surprisingly, the change in resistance is almost cancelled in the presence of light [32]. At low temperature, constant illumination completely quenches the effect of the electron bombardment, irrespective of any different surface treatment.

Since illumination with visible light can produce electron-hole excitations in the $Al_{0.24}Ga_{0.76}As/GaAs$ system, a naïve explanation of this remarkable effect could be that the additional carriers counterbalance the effect of the electric field produced by the surface charge. However, our explanation of the reversible photoconductivity invoking the existence of shallow traps is inconsistent with this simple mechanism. Moreover, two solid arguments stand against it:

i) The surface charge estimated according to our method (see Figs. 4B and 7B for the low and high temperature cases, respectively) is larger than the change in carrier density caused by illumination shown in the upper panels of Figure 3 for the low and high temperatures, respectively. Therefore, there would not be enough charge for this kind of compensation.

ii) If the counterbalancing effect took place, by decreasing the electron gun current, a threshold should be reached below which the surface charge is completely neutralized by the photoconductive (extra) charge. However, a simple experiment belies this idea. Figure 8 shows, as a function of the electron gun current, the surface charge density obtained from the change in resistance at room temperature, according to equation (1), for the light on and light off configurations. One can see that there is no drop to zero of the surface charge density for any gun current. Conversely, the differences in surface charge density between the light off and light on cases get smaller by decreasing the gun current. In the inset we plotted the ratio $(n^{\text{light off}} - n^{\text{light on}})/n^{\text{light off}}$ vs. current. This function is almost independent of the amount of the electron bombardment.

These findings support the following explanation: illumination directly photoionizes the surface charge. This process may be assisted by several factors, but it should definitely depend on the amount of charge that is actually deposited onto the surface. Indeed, the difference $n^{\text{light off}} - n^{\text{light on}}$ is nothing but the charge released into vacuum by photoemission, and must be proportional to the actual charge deposited, $n^{\text{light off}}$. We recall that the short time constants for the surface discharge led us to propose that the trapping proceeds only into metastable states generated by the image potential. In this regard

the action of light should be very efficient. From the inset of Figure 8 we infer an efficiency ϵ_{ph} for the photoionization process $\epsilon_{ph} = 0.82 \pm 0.02$. If the charge were permanently bound to the GaAs layer photoemission activated by visible light would not be possible, since the work function is $\simeq$4 eV. The work functions for Xe and ice are even larger. Therefore, the quenching effect due to light indirectly gives information on the maximum binding energy of the traps that are active.

4 Conclusions

We have demonstrated a novel method for studying the charging properties of a dielectric. To probe these, we monitor the conducting properties acquired or lost by an underlying system during the charging process. A representative example was provided by the study of the conductivity of the 2DEG in an $Al_{0.24}Ga_{0.76}As/GaAs$ quantum well structure, which was controlled by the surface electric field generated by surface charge deposited with an electron gun. Among the variety of applications to which this method could be applied, we have explored 1) the study of the metastability of the charged states and 2) the extent to which the conducting channel can be controlled.

In the former, we measured several discharging decay constants spanning the range between 0.2–10 s. From analysis of the fine features of the time recovery of the resistance at the turn off of the electron gun, we have proposed the existence of pure surface states (suggested to be trapped by the image potential) and states more deeply bound. We have not succeeded in obtaining permanent charging, irrespective of the the different treatments to which the surface was subjected. Possible reasons are the conditions of the surface, the ionizing action of black body radiation, and the energy of the electrons being too high. Unexpectedly, the charging seems to be less effective after the deposition of an ideal dielectric, such as Xe.

In general, a fair description of the build up of charge vs. time requires knowledge of the energy dependent sticking probability $\mu(E)$ and of the energy distribution of the secondary electrons which are beyond the reach of the present study. In any case, the transients observed in the charging behavior, although not fully reproducible, established a low efficiency for the charging process of $\simeq$0.1%.

We have detected a remarkable negative influence of illumination over the charging of the surface and proposed that the cause is photoemission of the metastable charge. We note that the quenching action of the light could be employed to reduce the switch off time of the conducting channel and thus increase the utility of the contactless gating in application devices.

With regards to the control of the transport properties via this method, we have been able to completely shut off the conductive channel under a suitable rate of irradiation. The *contactless gating* of the conductive channel could be useful whenever external constraints prevent the contamination of the surface with metal contacts, or when this is not recommended given the delicacy of a sample. In this regard, we intend to apply the method to relatively thin films ($L < 10\,\mu$m) of molecular crystals, such as C_{60}, perylene and pentacene.

Concerning the gating technique operated in this work, we are planning to extend the method of the contactless gating to other configurations, such as application of contacless metal plates connected to a DC or AC voltage power supply suspended at short distance ($L < 10\,\mu$m) from the sample.

This work was supported by: DOD/DARPA/DMEA (under Award No. DMEA90-02-2-0216). We also thank Brooke Erlanger, David Lidsky and James Cramer for help with setting up and debugging the instrumentation.

References

1. T. Martin, R. Bruinsma, P.M. Platzman, Phys. Rev. B **38**, 2257 (1988)
2. D.P. Clougherty, W. Kohn, Phys. Rev. B **46**, 4921 (1992)
3. W. Kohn, Surf. Rev. Lett. **1**, 129 (1994)
4. R.M. Marsolais, M. Deschenes, L. Sanche, Rev. Sci. Instrum. **60**, 2724 (1989); K. Nagesha, I.I. Fabricant, L. Sanche, J. Chem. Phys. **114**, 4934 (2001) and references therein
5. K. Nagesha, L. Sanche, Phys. Rev. Lett. **81**, 5892 (1998); A.D. Bass, L. Sanche, J. Chem. Phys. **95**, 2910 (1991), and references therein
6. W. Shockley, Phys. Rev. **56**, 317 (1939)
7. M.W. Cole, M.H. Cohen, Phys. Rev. Lett. **23**, 1238 (1969)
8. C.C. Grimes, G. Adams, Phys. Rev. Lett. **42**, 795 (1979)
9. E. Abrahams, S.V. Kravchenko, M.P. Sarachik, Rev. Mod. Phys. **73**, 251 (2001)
10. M. Pope, C.E. Swenberg, *Electronic Processes in Organic Crystals and Polymers*, 2nd edn. (Oxford Press, NY, 1999) p. 347
11. M. Biasini, R.D. Gann, J.A. Yarmoff, A.P. Mills Jr., L.N. Pfeiffer, K.W. West, X.P.A. Gao, B.C.D. Williams, Appl. Phys. Lett. **86**, 162111 (2005)
12. See, for example, K.W. Kolasinski, *Surface Science* (John Wiley & Sons LTD, 2002) p. 183–184
13. T. Koshikawa, R. Shimizu, K. Goto, K. Ishikawa, J. Phys. D Appl. Phys. **7**, 462 (1974)
14. R. Kollath, Ann. Phys.-Berlin **33**, 285 (1938)
15. Indeed, the earlier electron gun, allowing larger electron bombardment, succeeded to shut off completely the conductive channel. However, in the former case, the minimum filament bias required to observe any effect was for $V_b = -35$ V
16. Note that although we have investigated the composition of the gases injected in the chamber via residual gas analysis, we could not characterize the surface via Auger analysis and/or X-ray photoemission after its preparation. A modification of the experimental chamber will allow these diagnostics in the near future
17. N. Sakamoto, K. Hirakawa, T. Ikoma, Appl. Phys. Lett. **67**, 1444 (1995)
18. L.L. Chang, A. Koma, Appl. Phys. Lett. **29**, 138 (1976)
19. M. Zervos, M. Elliot, D.I. Westwood, Appl. Phys. Lett. **74**, 2026 (1999); E.P. De Poortere, Y.P. Shkolnikov, M. Shayegan, Phys. Rev. B **67**, 153303 (2003), and the references therein

20. D.J. Chadi, K.J. Chang, Phys. Rev. B **39**, 10063 (1989)
21. P.M. Mooney, J. Appl. Phys. **67**, R1 (1990), Figs 10, 11
22. A. Babinski, G. Li, C. Jagadish, Appl. Phys. Lett. **71**, 1664 (1997)
23. Note that, as mentioned above, this value is uncertain within the cool time of the halogen lamp
24. S.M. Sze, *Physics of Semiconductor devices* (John Wiley & Sons, 1969) pp. 29–30
25. See for example, S.V. Kravchenko, G.V. Kravchenko, J.E. Furneaux, V.M. Pudalov, M. D'Iorio, Phys. Rev. B **50**, 8039 (1994); X.P.A. Gao, A.P. Mills, A.P. Ramirez, L.N. Pfeiffer, K.W. West, Phys. Rev. Lett. **89**, 16801 (2002); E. Abrahams, S.V. Kravchenko, M.P. Sarachik, Rev. Mod. Phys. **73**, 251 (2001), and references therein
26. See, for example, F. Garnier, Philos. T. Roy. Soc. **355**, 815 (1997)
27. M.W. Cole, Phys. Rev. B **2**, 4239 (1970)
28. D. Straub, F.J. Himpsel, Phys. Rev. B **33**, 2256 (1986)
29. F.J. Himpsel, Phys. Rev. B **43**, 13394 (1991)
30. W.R. Merry, R.E. Jordan, D.F. Padowitz, C.B. Harris, Surf. Sci. **295**, 393 (1993)
31. As for the measurements shown in Figure 3, visible light was produced by a tungsten-halogen lamp
32. Note that the light on - light off resistances measured when the electron gun is off shown in Figure 7 are consistent with the results shown in Figure 3